

Quantum Vacuum Sagnac Effect

Guilherme C. Matos,¹ Reinaldo de Melo e Souza², Paulo A. Maia Neto^{1,*} and François Impens^{1,†}

¹*Instituto de Física, Universidade Federal do Rio de Janeiro, Rio de Janeiro, RJ, 21941-972, Brazil*

²*Instituto de Física, Universidade Federal Fluminense, Niterói, RJ, 24210-346, Brazil*

 (Received 19 August 2021; revised 6 October 2021; accepted 2 December 2021; published 29 December 2021)

We report on the quantum electrodynamical analog of a Sagnac phase induced by the fast rotation of a neutral nanoparticle onto atomic waves propagating in its vicinity. The quantum vacuum Sagnac phase is a geometric Berry phase proportional to the angular velocity of rotation. The persistence of a noninertial effect into the inertial frame is also analogous to the Aharonov-Bohm effect. Here, a rotation confined to a restricted domain of space gives rise to an atomic phase even though the interferometer is at rest with respect to an inertial frame. By taking advantage of a plasmon resonance, we show that the magnitude of the induced phase can be close to the sensitivity limit of state of the art interferometers. The quantum vacuum Sagnac atomic phase is a geometric footprint of a dynamical Casimir-like effect.

DOI: [10.1103/PhysRevLett.127.270401](https://doi.org/10.1103/PhysRevLett.127.270401)

The rotation of a frame attached to an interferometer with respect to an inertial frame induces an interferometric phase proportional to the angular frequency of the rotation and to the area enclosed by the interferometer. This phenomenon, known as the Sagnac effect [1], has several technological applications such as optical-based Sagnac sensors which have been embarked on aircraft for decades. Three decades ago, it was extended to matter waves [2]. Since then, cold-atom gyrometers based on the Sagnac effect [3,4] have been constantly improved to outperform their optical equivalents [5–9] (see Ref. [10] for a recent review).

We propose here to investigate the following closely related scheme—what if, instead of rotating the interferometer as a whole, one simply spins a neutral nanoparticle placed between its arms? Such a question naturally arises as rotation speeds beyond 5 GHz are achieved with optically levitated nanoparticles [11]. As in the Casimir effect, we show that the interaction between the atom and the nanoparticle mediated by the quantum electromagnetic field leads to an atomic phase induced by the particle’s spinning. We introduce the quantum vacuum Sagnac phase (QVSP) as an atom-interferometry footprint of noninertial effects in the quantum vacuum. The QVSP is thus analogous to the dynamical Casimir effect [12,13], but no real photons are emitted in the configuration discussed hereafter. Indeed, here the relative motions of the interfering wave packets with respect to the sense of the particle’s rotation plays a crucial role in the atom-particle interaction mediated by the quantum vacuum field. While dynamical Casimir photons are too scarce to be measurable [14–16] even when considering a cavity resonance [17–20], we show that the magnitude of the QVSP is close to the sensitivity limit of state-of-the-art atom interferometers [10,21] when taking into account the record rotation frequencies recently demonstrated with optically levitated nanoparticles [11,22,23].

The emission of dynamical Casimir photons out of the quantum vacuum state by a dielectric sphere undergoing a nonuniform rotation was considered in Ref. [24]. The electromagnetic field at finite temperature was predicted to exert a quantum friction torque on a neutral dispersive microsphere spinning at a constant rotation frequency [25,26]. The QVSP imprinted on the atomic center of mass (CM) provides an additional insight on how the rotation modifies the surrounding quantum electromagnetic field even when no real photons are emitted.

The QVSP is also a consequence of the motion of atomic CM with respect to the nanoparticle. In the context of atom interferometry, a nonlocal phase associated with pairs of paths (rather than with individual ones) was shown to result from the field-mediated interaction between a moving atom and a material surface [27–29]. Dynamical Casimir emission of photons [30–34], decoherence [35,36], and quantum friction [37–43] also result from the coupling between a moving atom and the quantum electromagnetic field. Given their high sensitivity, atom interferometers are candidates for the first experimental demonstration of motional effects in Casimir physics, and the QVSP would be particularly appealing for that purpose.

The QVSP is also related to the Aharonov-Bohm effect [44]. Such connection is well understood in the case of the standard Sagnac effect (see Ref. [45] for a recent review), as a rotating referential emulates the presence of magnetic fields thanks to the similarity between Coriolis and Lorentz forces [46]. This analogy has enabled the production of artificial effective magnetic fields in neutral cold-atom gases set into rotation [47]. Like the standard Sagnac phase, the QVSP is a geometric phase that can be cast in terms of an effective magnetic field. In addition, the QVSP can be seen as the Aharonov-Bohm-like counterpart of the Sagnac effect. Indeed, in the Aharonov-Bohm experiment,

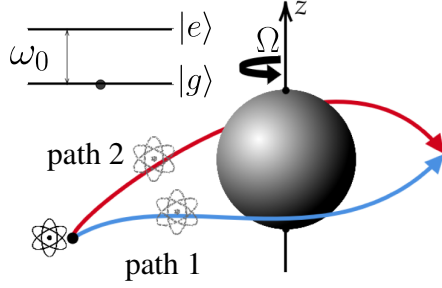


FIG. 1. Scheme of the quantum vacuum Sagnac interferometer. The center of mass of a ground-state atom propagates as a quantum superposition of two wave packets around a spinning neutral nanoparticle (angular frequency Ω).

a magnetic field confined to a solenoid imprints a phase in a region free of magnetic fields. Here, we show that a rotation confined to a domain of space imprints a phase on matter waves probing quantum vacuum fluctuations outside the rotating region.

For simplicity, we consider a nanoparticle rotating around an axis of symmetry with constant angular velocity Ω . In this case, the modification of the surrounding quantum field arises from the frequency dependence of the particle dielectric constant. We consider a two-level atom in the ground state interacting with the quantum vacuum field. The atom CM is in a quantum superposition of two wave packets that propagate in the vicinity of the spinning nanoparticle as indicated in Fig. 1. We show that the resulting QVSP is geometric, i.e., independent of the atomic velocity [48,49] in the limiting case of very narrow wave packets. Furthermore, we express the QVSP as the circulation of a geometric vector field, analog to the vector potential in the Aharonov-Bohm effect, along the interferometer paths. The effect can be enhanced by considering nanoparticles with a plasmon resonance [50] in order to optimize the material dispersion at the atomic transition frequency.

Motional van der Waals (vdW) atomic phase.—We consider a moving atom interacting with the rotating nanoparticle between the initial and final times $t = \mp T/2$. The atomic waves acquire a phase associated with the dipolar interaction $\hat{H}_{\text{dip}} = -\hat{\mathbf{d}} \cdot \hat{\mathbf{E}}$, with $\hat{\mathbf{d}}$ representing the atomic dipole moment operator. The electric field operator $\hat{\mathbf{E}}$ is taken at the instantaneous average atomic position $\mathbf{r}_k(t) = \langle \hat{\mathbf{r}}(t) \rangle_k$ for each wave packet k . We evaluate the phase difference $\Delta\phi_{12}$ accumulated by the coherent superposition state of two narrow atomic wave packets following the two distinct paths $\mathcal{P}_1 = [\mathbf{r}_1(t)]$, $\mathcal{P}_2 = [\mathbf{r}_2(t)]$. Up to second order in perturbation theory, this phase difference reads [29]

$$\Delta\phi_{12} = \varphi_{11} - \varphi_{22} + \varphi_{12} - \varphi_{21}, \quad (1)$$

$$\begin{aligned} \varphi_{kl} = \frac{1}{4} \iint_{-T/2}^{T/2} dt dt' \{ & g_{\mathbf{a}}^H(t, t') \mathcal{G}_{\hat{\mathbf{E}}}^{R,S}[\mathbf{r}_k(t), t; \mathbf{r}_l(t'), t'] \\ & + g_{\mathbf{a}}^R(t, t') \mathcal{G}_{\hat{\mathbf{E}}}^{H,S}[\mathbf{r}_k(t), t; \mathbf{r}_l(t'), t'] \}. \end{aligned} \quad (2)$$

The contributions φ_{kl} for $k = l$ and $k \neq l$ correspond to local and nonlocal phases, respectively. In the concrete applications discussed later on, the local phases $\phi_k \equiv \varphi_{kk}$ will play a more important role. We have used the trace of the retarded Green's function for the scattered electric field $\mathcal{G}_{\hat{\mathbf{E}}}^{R,S}(\mathbf{r}, t; \mathbf{r}', t') = \text{Tr}[\mathbf{G}_{\hat{\mathbf{E}}}^{R,S}(\mathbf{r}, t; \mathbf{r}', t')]$, which captures how electro-dynamical propagation is modified by the presence of the nanoparticle (scatterer) placed at the origin. Likewise, the trace $\mathcal{G}_{\hat{\mathbf{E}}}^{H,S}$ of the Hadamard Green's function represents the change in the field fluctuations induced by the presence of the nanoparticle. The retarded Green's function of a vectorial operator $\hat{\mathbf{O}}(t)$ is defined as the averaged commutator $\mathbf{G}_{\hat{\mathbf{O}}_{ij}}^R(t, t') = (i/\hbar)\Theta(t-t')\langle [\hat{O}_i(t), \hat{O}_j(t')] \rangle$ with $\Theta(t)$ denoting the Heaviside function. The Hadamard Green's function corresponds to the average value of the anticommutator $\mathbf{G}_{\hat{\mathbf{O}}_{ij}}^H(t, t') = (1/\hbar)\langle \{ \hat{O}_i(t), \hat{O}_j(t') \} \rangle$.

The first term on the rhs of (2) accounts for the electric field response to dipole fluctuations, while the second one corresponds to the dipole response to vacuum fluctuations modified by the presence of the nanoparticle. The dipole Hadamard Green's function is isotropic and has the analytical form $g_{\mathbf{a}ij}^H(t, t') = \alpha_0^A \omega_0 \cos \omega_0(t-t') \delta_{ij}$ for a two-level model. Here, α_0^A represents the static polarizability and ω_0 is the transition frequency. We focus on the nonretarded vdW regime, for which the atom-particle distance $r(t)$ is much smaller than the transition wavelength $\lambda_0 = 2\pi c/\omega_0$. As shown below, the QVSP is maximized in the immediate vicinity of the rotating nanoparticle, which turns the vdW regime more interesting for experimental implementations.

We now consider the retarded Green's function for the scattered electric field $\mathbf{G}_{\hat{\mathbf{E}}ij}^{R,(S)}(\mathbf{r}, t; \mathbf{r}', t')$. This function corresponds to the i th component of the electric field at position \mathbf{r} and time t induced by an instantaneous point dipole oriented along the j th direction at position \mathbf{r}' and time t' after scattering at the nanoparticle at some intermediate time t'' such that $t' < t'' < t$. From now on, we assume that the nanoparticle is very small and neglect multipolar contributions beyond the electric dipolar one. The retarded Green's function in the frequency domain can then be expressed in terms of the electric polarizability tensor $\alpha^\Omega(\omega)$ of the rotating nanoparticle as

$$\mathbf{G}_{\hat{\mathbf{E}}}^{R,S}(\mathbf{r}, \mathbf{r}', \omega) = \mathbf{G}^0(\mathbf{r}, \mathbf{0}, \omega) \cdot \alpha^\Omega(\omega) \cdot \mathbf{G}^0(\mathbf{0}, \mathbf{r}', \omega). \quad (3)$$

The free-space retarded Green's function for the electric field becomes frequency independent [51] $\mathbf{G}_{ij}^0(\mathbf{r}, \mathbf{r}', \omega) \approx (3R_i R_j / R^2 - \delta_{ij}) / (4\pi\epsilon_0 R^3)$ in the nonretarded vdW regime ($\mathbf{R} = \mathbf{r} - \mathbf{r}'$). In the absence of rotation, any direction orthogonal to the symmetry axis of the nanoparticle is a principle axis of the polarizability tensor $\alpha^0(\omega)$ with an eigenvalue denoted by $\tilde{\alpha}(\omega)$. Rotation around the symmetry

axis leads to a nondiagonal correction $\delta\alpha^\Omega(\omega)_{lm} = \alpha^\Omega_{lm}(\omega) - \alpha^0_{lm}(\omega) \approx i\tilde{\alpha}'(\omega) \sum_n \epsilon_{lmn} \Omega_n$ [25] which lies at the heart of the QVSP. We have assumed a nonrelativistic rotation with angular velocity Ω , $\tilde{\alpha}'(\omega)$ is the frequency derivative of the polarizability eigenvalue, and ϵ_{lmn} denotes the Levi-Civita tensor components.

QVSP induced by a rotating nanoparticle.—We provide first a heuristic discussion of the QVSP derived below. This phase arises from the scattering of virtual photons on the spinning nanoparticle, which carry back to the atom a trace of the particle rotation. The QVSP captures the noninertial footprint on the quantum electromagnetic field as the atom probes fluctuations in the vicinity of the particle. In this sense, it constitutes a *dynamical Casimir-like* effect. However, as a nanoparticle spinning at constant velocity produces no radiation [24,25], the QVSP does not rely on the presence of real dynamical Casimir photons—nor does it rests on open-quantum system dynamics [52] responsible for quantum friction [41,43].

The problem under consideration involves very different time scales, listed below from the slowest to the fastest in the vdW regime: the time-of-flight T of the atomic CM in the vicinity of the rotating particle, the period of rotation (a fraction of nanoseconds), the inverse of the atomic transition frequency $2\pi/\omega_0$, the response time of the rotating particle due to dispersion, and finally the light travel time between the moving atom and the particle, r/c . Such hierarchy of time scales allows us to take several approximations. The dominant contribution in Eq. (2) comes from intervals $t - t'$ of the order of the response time of the nanoparticle, enabling us to neglect the CM acceleration and take $\mathbf{r}_k(t') \simeq \mathbf{r}_k(t) - (t - t')\mathbf{v}_k(t)$ in Eqs. (2) and (3).

In addition, the displacement of the atomic CM during $t - t'$ is much smaller than the wavelengths of field modes contributing to the electric field Green's functions. Thus, we Taylor expand the latter around the position $\mathbf{r}_k(t)$. We start by deriving the local contribution to the QVSP and define ϕ_k^Ω as the Ω -dependent contribution to the phase ϕ_k in Eq. (2). We write it as the sum $\phi_k^\Omega = \phi_{\text{qs},k}^\Omega + \phi_{\text{mot},k}^\Omega$ of a quasistatic and of a motional contribution. The former is obtained by taking identical arguments for the retarded and advanced positions [$\mathbf{r} = \mathbf{r}' = \mathbf{r}_k(t)$] in the electric Green's function, while the latter involves instead the gradient of the Green's functions and the instantaneous atomic CM velocity.

The quasistatic contribution $\phi_{\text{qs},k}^\Omega$ vanishes by symmetry considerations [53]. The QVSP thus arises exclusively from the atomic motion during the electro-dynamical delay time $t - t'$ associated with the exchange of virtual photons between the atom and the nanoparticle. We write $\phi_k^\Omega = \phi_{\text{mot},k}^\Omega = \phi_k^{\Omega,\text{dip}} + \phi_k^{\Omega,f}$ as the sum of contributions from dipole and field fluctuations, respectively. They correspond

to the first and second terms in Eq. (2). We use the condition $\omega_0 T \gg 1$ to derive

$$\phi_k^{\Omega,\text{dip}} = -\frac{\omega_0 \alpha_0^A}{4} \int_{-T/2}^{T/2} dt \mathbf{v}_k(t) \cdot \partial_\omega \nabla_{\mathbf{r}'} \text{Im}[\delta\mathcal{G}_{\mathbf{E}}^{R,S}(\mathbf{r}, \mathbf{r}'; \omega)], \quad (4)$$

where the spatial and frequency derivatives are taken at $\mathbf{r}' = \mathbf{r} = \mathbf{r}_k(t)$ and $\omega = \omega_0$, respectively. Here, $\delta\mathcal{G}_{\mathbf{E}}^{R,S}$ represents the Ω -dependent contribution to the scattered Green function, which is obtained by taking $\delta\alpha^\Omega(\omega)$ instead of the full tensor $\alpha(\omega)$ in Eq. (3). The frequency derivative captures the time delay associated with the nanoparticle response to the field (in the form of an induced dipole) during the atomic motion. On the other hand, the delay associated with the light propagation time from the atom to the nanoparticle is negligible within the vdW approximation. Accordingly, we take the nonretarded vdW approximation for the free-space Green's function $\mathbf{G}^0(\mathbf{r}, \mathbf{r}', \omega)$ when deriving the scattered field propagator $\delta\mathcal{G}_{\mathbf{E}}^{R,S}(\mathbf{r}, \mathbf{r}'; \omega)$ from Eq. (3).

The contribution from field fluctuations $\phi_k^{\Omega,f}$ is given by an expression similar to (4) in terms of the retarded Green's function for the dipole (polarizability) and the Hadamard Green's function for the field. Using the fluctuation-dissipation theorem $\nabla_{\mathbf{r}'} \mathcal{G}_{\mathbf{E}}^{H,S}(\mathbf{r}, \mathbf{r}'; \omega) = 2\text{sgn}(\omega) \text{Im}[\nabla_{\mathbf{r}'} \mathcal{G}_{\mathbf{E}}^{R,S}(\mathbf{r}, \mathbf{r}'; \omega)]$, with $\text{sgn}(\omega)$ denoting the sign function, we find a contribution to the local QVSP identical to the dipolar one. We write the final result for the local QVSP as a geometric integral [53], which is the main result of this Letter:

$$\phi_k^\Omega = \frac{9}{2} \frac{\omega_0 \alpha_0^A \tilde{\alpha}'_R(\omega_0)}{(4\pi\epsilon_0)^2} \int_{\mathcal{P}_k} d\mathbf{r} \cdot \frac{\Omega \times \mathbf{r}}{r^8}, \quad (5)$$

where $\tilde{\alpha}_R$ is the real part of the nanoparticle's polarizability eigenvalue. The integral is performed along the interferometer path \mathcal{P}_k delimited by the initial and final positions $\mathbf{r}_k(\mp T/2)$. As in the standard Sagnac effect [46,47], the QVSP given by Eq. (5) is a geometric phase that can be cast as the line integral of an effective vector potential proportional to the angular velocity Ω . The QVSP (5) possess all the distinctive features of a geometric phase: it is independent of the velocity magnitude, but changes sign when the direction of propagation is reversed.

As an important insight in its geometric nature, one can show [53] that the QVSP is indeed a Berry phase [54,55] of the full quantum system “two-level atom+field” undergoing a unitary and adiabatic quantum evolution steered by the atomic position. Because of the dipole interaction, the instantaneous ground state of this quantum system changes continuously as the atom propagates nearby the spinning nanoparticle, following a quantum trajectory which depends on the interferometer path. By integrating the corresponding Berry connection, one retrieves exactly the local QVSP (5).

The correction associated with electro-dynamical retardation is given by [53] $\phi_{(c),k}^\Omega = 3\omega_0 \alpha_0^A \tilde{\alpha}'_R(\omega_0) / [(4\pi\epsilon_0)^2 c^2] \int_{\mathcal{P}_k} d\mathbf{r} \cdot [(\Omega \times \mathbf{r})/r^6]$ and is negligible for the

example discussed below. In the case of a finite temperature θ , the local QVSP is multiplied by the factor $\coth(\hbar\omega_0/2k_B\theta)$ ($k_B =$ Boltzmann constant), which is very close to one for any realistic example of atomic transition. In other words, the contribution from thermal fluctuations is negligible and the QVSP is a genuine quantum vacuum effect.

Examples of interferometer designs.—To illustrate our findings, we calculate the phase for two specific geometries: either a circle of radius R centered on the nanoparticle, or two parallel straight lines enclosing the particle. In both cases we assume that $\mathbf{\Omega} = \Omega\hat{z}$ is orthogonal to the plane containing the trajectories. The first arrangement is a textbook example of a Sagnac interferometer, whereas the latter corresponds to a more realistic situation in atom interferometry [56–58]. One finds $\phi_{\{r=R\}}^{\Omega} = 9\pi\ell_{\Omega}^6/R^6$ for the circular trajectory when the senses of rotation of atom and nanoparticle coincide; and $\phi_{\{x=x_1, -L/2 \leq y \leq L/2, z=z_1\}}^{\Omega} \approx 45\pi\ell_{\Omega}^6 x_1 / (32r_{\perp}^7)$ with $r_{\perp} = (x_1^2 + z_1^2)^{1/2}$ for a straight segment of length L satisfying the condition $|x_1|, |z_1| \ll L/2 \ll \lambda_0$ for consistency with the vdW approximation. We have introduced the characteristic length scale $\ell_{\Omega} = [\omega_0\alpha_0\alpha_R''(\omega_0)\Omega/(4\pi\epsilon_0)^2]^{1/6}$.

Nonlocal contributions to the QVSP difference.—We now discuss the nonlocal QVSP contribution $\phi_{12}^{\Omega} - \phi_{21}^{\Omega}$ corresponding to the Ω -dependent part of the nonlocal phases in Eq. (1). In a different context, cross talks of the interferometer paths can influence significantly the motional phases [27–29] or decoherence rates [35,59] induced by the quantum vacuum. While the nonlocal QVSP difference vanishes for circular trajectories, it is nonzero when considering two parallel straight-line trajectories with the nanoparticle at the midpoint ($x_2 = -x_1$ and $z_1 = z_2 = 0$). In this case, the nonlocal QVSP contribution has an opposite sign with respect to the local one, thus reducing the total QVSP difference to $\Delta\phi_{12}^{\Omega} = 63\pi\ell_{\Omega}^6 \text{sgn}(x_1)/(32x_1^6)$. For this geometry, the nonlocal contribution represents a sizable part of the total QVSP difference.

Estimation of the QVSP for finite-width atomic wave packets and a spherical nanoparticle.—We estimate the magnitude of the QVSP in a practical interferometer implementation. Specifically, we consider a Mach-Zehnder configuration where path 1 flies near a rotating nanosphere of radius a , and path 2 evolves far away from the nanosphere. A similar interferometer geometry was used in [56–58] for the measurement of quasistatic vdW phases. In this setup, the QVSP receives only a local contribution from path 1, namely $\Delta\phi_{12}^{\Omega} = \phi_1^{\Omega}$. In order to enhance the QVSP, we investigate materials for which the polarizability exhibits a sharp frequency dependence at the atomic transition frequency.

For this purpose, we use a plasmon resonance [50] and seek metals for which the polarizability $\tilde{\alpha}(\omega) = (4\pi\epsilon_0)a^3[\epsilon(\omega) - 1]/[\epsilon(\omega) + 2]$ is maximized by reducing

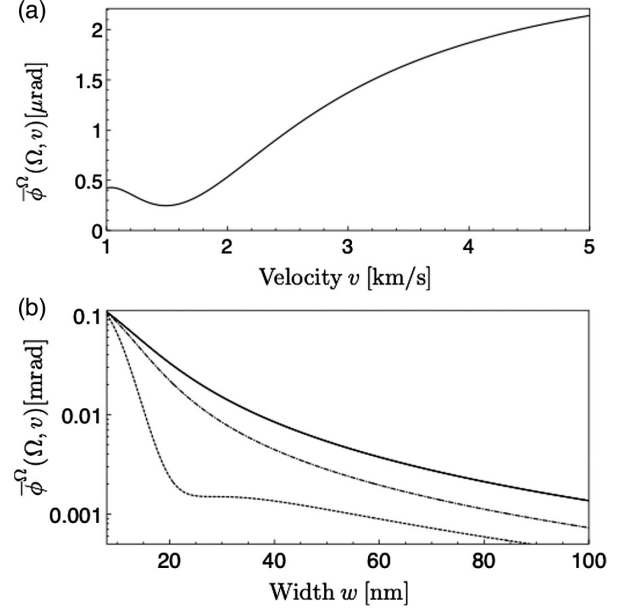


FIG. 2. Average QVSP versus (a) velocity and (b) width of the Gaussian atomic beam used in the interferometer. Parameters: (a) $a = 50$ nm, $w = 100$ nm. (b) $a = 35$ nm, $v = 3$ km/s (dotted line), $v = 4$ km/s (dash-dotted line) and $v = 5$ km/s (solid line). In (a),(b) we have considered a two-level Na atom with the static polarizability $\alpha_0^A = (4\pi\epsilon_0) \times 2.4 \times 10^{-29}$ m³ and transition frequency $\omega_0 = 3.198 \times 10^{15}$ rad/s. We have taken a nanosphere of potassium spinning at the angular velocity $\Omega = 2\pi \times 5$ GHz.

$\epsilon(\omega) + 2$ at the atomic transition frequency ω_0 . Within the Drude model, the dielectric constant reads $\epsilon(\omega) = 1 - \omega_p^2/[\omega(\omega + i\gamma)]$, where ω_p is the plasma frequency and γ is the inverse of the electronic relaxation time. The plasma resonance in the dipole approximation is at $\omega_{\text{res}} = \omega_p/\sqrt{3}$. Since we want to maximize $\tilde{\alpha}_R''(\omega)$ rather than $\tilde{\alpha}'(\omega)$, we need the atomic transition frequency to be slightly shifted with respect to ω_{res} . We consider Na atoms, for which the static polarizability is $\alpha_0^A/(4\pi\epsilon_0) = 2.4 \times 10^{-29}$ m³ and the dominant transition ($3s_{1/2} - 3p_{3/2}$) has a frequency $\omega_0 = 3.198 \times 10^{15}$ rad/s [60]. We take the plasma frequency of the nanosphere to be $\omega_p = 5.549 \times 10^{15}$ rad/s so as to maximize $\tilde{\alpha}_R''(\omega_0)$. Such fine tuning can be achieved, for instance, from the size dependence of the plasmon resonance in nanospheres [61,62]. Our value for ω_p is also very close, within less than 1%, to the bulk plasma frequency of potassium [63]. Accordingly, we take the relaxation frequency of potassium $\gamma = 2.795 \times 10^{13}$ rad/s in our numerical estimation (Fig. 2).

We average the atomic phase over the transverse wave packet widths following the procedure of Refs. [56–58] for (quasistatic) vdW phases. The phase acquired by atoms flying along the trajectory $\{x' = x, -L/2 \leq y' \leq L/2, z' = z\}$ at a constant velocity $\mathbf{v} = v\hat{y}$, is the sum of the vdW phase $\phi^{\text{vdW}}(x, z, v)$, as derived by integration of the instantaneous vdW potential along the trajectory, and the QVSP $\phi^{\Omega}(x, z)$:

$\phi(\Omega, x, z, v) = \phi^{\text{vdW}}(x, z, v) + \phi^\Omega(x, z)$. The known result [56] for the vdW phase follows from Eqs. (2) and (3) in the quasistatic limit: $\phi^{\text{vdW}}(x, z, v) \simeq 9\pi\alpha_0\omega_0\tilde{\alpha}_R(\omega_0)/[4.(4\pi\epsilon_0)^2vr_\perp^5]$ with $r_\perp = (x^2 + z^2)^{1/2}$. There are two important differences between the vdW phase and the QVSP. The former is dynamical and thus inversely proportional to the velocity, while the latter is geometric and thus velocity independent. On the other hand, the vdW phase is unaffected by the nanosphere's spinning, while the QVSP is proportional to the angular velocity Ω .

The experimentally accessible phase reads $\bar{\phi}(\Omega, v) = \arctan[\sin[\phi(\Omega, x, z, v)]/\cos[\phi(\Omega, x, z, v)]]$, where the averaging is performed over the transverse coordinates x, z . We consider a Gaussian atomic wave packet of transverse width w and longitudinal velocity v . In practice, one may gradually increase the nanosphere rotation in order to isolate the average QVSP as the Ω -dependent part of the total average phase: $\bar{\phi}^\Omega(\Omega, v) \equiv \bar{\phi}(\Omega, v) - \bar{\phi}(0, v)$. In spite of the geometric nature of $\phi^\Omega(x, z)$, the presence of the dynamical phase $\phi^{\text{vdW}}(x, z, v)$ together with the averaging procedure involving trigonometric functions turn $\bar{\phi}^\Omega(\Omega, v)$ velocity dependent in the case of finite-width wave packets.

We take the angular velocity $\Omega = 2\pi \times 5$ GHz recently achieved with optically levitated nanoparticles [11]. We also consider thin atomic beams of width $w \leq 100$ nm centered at the edge of the spinning particle. Such collimation may be obtained by using diffraction through a nanograting [58] placed in the vicinity of the spinning particle, or by tight focusing techniques considered for atom lithography [64]. Prospective focusing techniques [65,66] show indeed that atomic beam widths $w \simeq 8$ nm may be attained. We plot $\bar{\phi}^\Omega(\Omega, v)$ versus velocity in Fig. 2(a) for a nanosphere of radius $a = 50$ nm and an atomic wave packet of width $w = 100$ nm. Figure 2(b) presents the variation of $\bar{\phi}^\Omega(\Omega, v)$ with the wave packet width, for $a = 35$ nm and for different velocities of a few km/s. The averaged QVSP tends to increase with the atomic velocity and is enhanced by atomic beam focusing. However, $\bar{\phi}^\Omega(\Omega, v)$ may be significantly attenuated around specific velocities or width values under the influence of the quasistatic vdW phase. To avoid the detrimental effect of the vdW potential, we consider fast atomic beams, with velocities comparable to those of Ref. [58]. Figure 2(b) shows that an average QVSP $\bar{\phi}^\Omega(\Omega, v) \simeq 0.1$ mrad is attained for $w = 8$ nm. Such value is close to the current phase sensitivity limit in atom interferometry [10,67].

Conclusions.—We have shown that the fast rotation of a nanoparticle imprints a geometric phase analogous to a Sagnac phase on a ground-state atom propagating in its vicinity. The persistence of a noninertial effect beyond the region where the rotation actually occurs is reminiscent of the Aharonov-Bohm effect, with the vector potential yielding a finite atomic phase in a region free of magnetic field. We have assumed the interferometer to be at rest with

respect to an inertial frame. Thus, the noninertial effects are exclusively mediated by the quantum vacuum field through the scattering on a rotating nanoparticle. The resulting QVSP is a dynamical Casimir-like modification of the atomic phase, whose observation might be more at hand than the detection of dynamical Casimir photons. Quantum dipolar and field fluctuations contribute equally to the QVSP, which can be enhanced by using materials exhibiting a plasmon resonance near the atomic transition frequency. The QVSP might become within reach of experimental observation given the state of the art in atom interferometry and nanorotors.

F. I. thanks Jean Dalibard for stimulating initial discussions, and A. Z. Khoury, M. B. da Silva Neto for discussions on geometric phases. F. I. and P. A. M. N. are grateful to Ryan O. Behunin and Claudio Ccappa Tira for a previous collaboration on nonlocal atomic phases. We acknowledge funding from the Brazilian agencies Conselho Nacional de Desenvolvimento Científico e Tecnológico (CNPq) (409994/2018-9), Coordenação de Aperfeiçoamento de Pessoal de Nível Superior (CAPES), and Fundação de Amparo à Pesquisa do Estado do Rio de Janeiro (FAPERJ) (202.874/2017, 210.242/2018 and 210.296/2019). P. A. M. N. also thanks partial financial support from Instituto Nacional de Ciência e Tecnologia de Fluidos Complexos (INCT-FCx) and Fundação de Amparo à Pesquisa do Estado de São Paulo (FAPESP) (2014/50983-3).

*Corresponding author.

pamn@if.ufrj.br

†Corresponding author.

impens@if.ufrj.br

- [1] G. Sagnac, C.R. Hebd. Seances Acad. Sci. **141**, 1220 (1913); **157**, 708 (1913).
- [2] Ch. J. Bordé, *Phys. Lett.* **140A**, 10 (1989).
- [3] T. L. Gustavson, P. Bouyer, and M. A. Kasevich, *Phys. Rev. Lett.* **78**, 2046 (1997).
- [4] A. Lenef, T. D. Hammond, E. T. Smith, M. S. Chapman, R. A. Rubenstein, and D. E. Pritchard, *Phys. Rev. Lett.* **78**, 760 (1997).
- [5] B. Canuel, F. Leduc, D. Holleville, A. Gauguet, J. Fils, A. Viridis, A. Clairon, N. Dimarcq, Ch. J. Bordé, A. Landragin, and P. Bouyer, *Phys. Rev. Lett.* **97**, 010402 (2006).
- [6] A. D. Cronin, J. Schmiedmayer, and D. E. Pritchard, *Rev. Mod. Phys.* **81**, 1051 (2009).
- [7] E. R. Moan, R. A. Horne, T. Arpornthip, Z. Luo, A. J. Fallon, S. J. Berl, and C. A. Sackett, *Phys. Rev. Lett.* **124**, 120403 (2020).
- [8] C. Ryu, E. C. Samson, and M. G. Boshier, *Nat. Commun.* **11**, 3338 (2020).
- [9] C. Schubert, S. Abend, M. Gersemann, M. Gebbe, D. Schlippert, P. Berg, and E. M. Rasel, *Sci. Rep.* **11**, 16121 (2021).
- [10] R. Geiger, A. Landragin, S. Merlet, and F. Pereira Dos Santos, *AVS Quantum Sci.* **2**, 024702 (2020).

- [11] J. Ahn, Z. Xu, J. Bang, P. Ju, X. Gao, and T. Li, *Nat. Nanotechnol.* **15**, 89 (2020).
- [12] D. A. R. Dalvit, P. A. Maia Neto, and F. D. Mazzitelli, *Lect. Notes Phys.* **834**, 287 (2011).
- [13] M. Fernandez-Serra, *Physics* **2**, 67 (2009).
- [14] P. A. Maia Neto and L. A. S. Machado, *Phys. Rev. A* **54**, 3420 (1996).
- [15] L. Woods, M. Krüger, and V. V. Dodonov, *Appl. Sci.* **11**, 293 (2021).
- [16] D. A. R. Dalvit and W. Kort-Kamp, *Universe* **7**, 189 (2021).
- [17] A. Lambrecht, M.-T. Jaekel, and S. Reynaud, *Phys. Rev. Lett.* **77**, 615 (1996).
- [18] V. V. Dodonov and A. B. Klimov, *Phys. Rev. A* **53**, 2664 (1996).
- [19] R. Schützhold, G. Plunien, and G. Soff, *Phys. Rev. A* **57**, 2311 (1998).
- [20] M. Crocce, D. A. R. Dalvit, and F. D. Mazzitelli, *Phys. Rev. A* **64**, 013808 (2001).
- [21] T. Kumiya, A. S. Akent'ev, Y. Mori, J. Ichimura, and A. Morinaga, *Phys. Rev. A* **93**, 023637 (2016).
- [22] R. Reimann, M. Doderer, E. Hebestreit, R. Diehl, M. Frimmer, D. Windey, F. Tebbenjohanns, and L. Novotny, *Phys. Rev. Lett.* **121**, 033602 (2018).
- [23] J. Ahn, Z. Xu, J. Bang, Y.-H. Deng, T. M. Hoang, Q. Han, R.-M. Ma, and T. Li, *Phys. Rev. Lett.* **121**, 033603 (2018).
- [24] G. Barton, *Ann. Phys. (N.Y.)* **245**, 361 (1996).
- [25] A. Manjavacas and F. J. García de Abajo, *Phys. Rev. A* **82**, 063827 (2010).
- [26] A. Manjavacas and F. J. García de Abajo, *Phys. Rev. Lett.* **105**, 113601 (2010).
- [27] F. Impens, R. O. Behunin, C. C. T'ira, and P. A. Maia Neto, *Eur. Phys. Lett.* **101**, 60006 (2013).
- [28] F. Impens, C. C. T'ira, and P. A. Maia Neto, *J. Phys. B* **46**, 245503 (2013).
- [29] F. Impens, C. C. T'ira, R. O. Behunin, and Paulo A. Maia Neto, *Phys. Rev. A* **89**, 022516 (2014).
- [30] R. M. Souza, F. Impens, and Paulo A. Maia Neto, *Phys. Rev. A* **97**, 032514 (2018).
- [31] L. Z. Lo and C. K. Law, *Phys. Rev. A* **98**, 063807 (2018).
- [32] M. B. Fariás, C. D. Fosco, F. C. Lombardo, and F. D. Mazzitelli, *Phys. Rev. D* **100**, 036013 (2019).
- [33] B. P. Dolan, A. Hunter-McCabe, and J. Twamley, *New J. Phys.* **22**, 033026 (2020).
- [34] A. Agustí, L. García-Álvarez, E. Solano, and C. Sabín, *Phys. Rev. A* **103**, 062201 (2021).
- [35] S. Scheel and S. Y. Buhmann, *Phys. Rev. A* **85**, 030101(R) (2012).
- [36] R. Melo Souza, F. Impens, and Paulo A. Maia Neto, *Phys. Rev. A* **94**, 062114 (2016).
- [37] S. Scheel and S. Y. Buhmann, *Phys. Rev. A* **80**, 042902 (2009).
- [38] G. Pieplow and C. Henkel, *New J. Phys.* **15**, 023027 (2013).
- [39] M. Donaire and A. Lambrecht, *Phys. Rev. A* **93**, 022701 (2016).
- [40] D. Reiche, F. Intravaia, J.-T. Hsiang, K. Busch, and B. L. Hu, *Phys. Rev. A* **102**, 050203(R) (2020).
- [41] M. B. Fariás, F. C. Lombardo, A. Soba, P. I. Villar, and R. S. Decca, *npj Quantum Inf.* **6**, 25 (2020).
- [42] C. D. Fosco, F. C. Lombardo, and F. D. Mazzitelli, *Universe* **7**, 158 (2021).
- [43] F. C. Lombardo, R. S. Decca, L. Viotti, and P. I. Villar, *Adv. Quant. Tech.* **4**, 2000155 (2021).
- [44] Y. Aharonov and D. Bohm, *Phys. Rev.* **115**, 485 (1959).
- [45] I. L. Paiva, R. Lenny, and E. Cohen, [arXiv:2110.05824](https://arxiv.org/abs/2110.05824).
- [46] J. Dalibard, F. Gerbier, G. Juzeliūnas, and P. Öhberg, *Rev. Mod. Phys.* **83**, 1523 (2011).
- [47] V. Schweikhard, I. Coddington, P. Engels, V. P. Mogendorff, and E. A. Cornell, *Phys. Rev. Lett.* **92**, 040404 (2004).
- [48] Ch. Miniatura, J. Robert, O. Gorceix, V. Lorent, S. Le Boiteux, J. Reinhardt, and J. Baudon, *Phys. Rev. Lett.* **69**, 261 (1992).
- [49] J. Gillot, S. Lepoutre, A. Gauguet, M. Büchner, and J. Vigué, *Phys. Rev. Lett.* **111**, 030401 (2013).
- [50] J. A. Scholl, A. L. Koh, and J. A. Dionne, *Nature (London)* **483**, 421 (2012).
- [51] W. Heitler, *The Quantum Theory of Radiation* (Dover, New York, 1954), Chap. II.
- [52] F. C. Lombardo and P. I. Villar, *Phys. Rev. A* **74**, 042311 (2006).
- [53] See Supplemental Material at <http://link.aps.org/supplemental/10.1103/PhysRevLett.127.270401> for a detailed derivation of the QVSP and of the associated Berry connection.
- [54] M. V. Berry, *Proc. R. Soc. A* **392**, 45 (1984).
- [55] A. Shapere and F. Wilczek, *Geometric Phases in Physics* (World Scientific, Singapore, 1989).
- [56] A. D. Cronin and J. D. Perreault, *Phys. Rev. A* **70**, 043607 (2004).
- [57] S. Lepoutre, H. Jelassi, V. P. A. Lonij, G. Tréneç, M. Büchner, A. D. Cronin, and J. Vigué, *Eur. Phys. Lett.* **88**, 20002 (2009).
- [58] S. Lepoutre, V. P. A. Lonij, H. Jelassi, G. Tréneç, M. Büchner, A. D. Cronin, and J. Vigué, *Eur. Phys. J. D* **62**, 309 (2011).
- [59] Francisco D. Mazzitelli, Juan Pablo Paz, and Alejandro Villanueva, *Phys. Rev. A* **68**, 062106 (2003).
- [60] W. F. Holmgren, M. C. Revelle, V. P. A. Lonij, and A. D. Cronin, *Phys. Rev. A* **81**, 053607 (2010).
- [61] A. Derkachova, K. Kolwas, and I. Demchenko, *Plasmonics* **11**, 941 (2016).
- [62] S. Karimi, A. Moshaii, S. Abbasian, and M. Nikkhah, *Plasmonics* **14**, 851 (2019).
- [63] M. G. Blaber, M. D. Arnold, and M. J. Ford, *J. Phys. Chem. C* **113**, 3041 (2009).
- [64] G. Timp, R. E. Behringer, D. M. Tennant, J. E. Cunningham, M. Prentiss, and K. K. Berggren, *Phys. Rev. Lett.* **69**, 1636 (1992).
- [65] R. Richberg, S. S. Szigeti, and A. M. Martin, *Phys. Rev. A* **103**, 063304 (2021).
- [66] R. Richberg and A. M. Martin, *Phys. Rev. A* **104**, 033314 (2021).
- [67] L. Salvi, N. Poli, V. Vuletić, and G. M. Tino, *Phys. Rev. Lett.* **120**, 033601 (2018).